Synthesis and Characterization of Reduced Graphene Oxide Iron Oxide Tin Oxide Nanocomposites for Biological Applications in Water Treatment

Ali Fadhil Ismail and Entisar E. Al-Abodi
Department of Chemistry, College of Education for Pure Science -Ibn-Al-Haitham, University of Baghdad, 00964 Baghdad, Iraq
{entisar.a.1, ali.fadel2205p}@ihcoedu.uobaghdad.edu.iq

Keywords: Nanocomposites, Tin Dioxide, Biological Activity, Microorganisms.

Abstract: In this study, the synthesis, characterization, and biological applications of rGO/Fe_3O_4/SnO_2 nanocomposites are discussed for water treatment. The synthesis was conducted via a modified Hummer's method to obtain reduced graphene oxide (rGO), followed by the incorporation of Fe_3O_4 and SnO_2 nanoparticles through a facile co-precipitation process. Various characterization techniques, including Fourier-transform infrared spectroscopy (FT-IR), X-ray diffraction (XRD), field emission scanning electron microscopy (FESEM), and energy-dispersive X-ray spectroscopy (EDX), confirmed successful formation and structural integrity of the nanocomposites. The morphological analysis revealed uniform dispersion of Fe_3O_4 and SnO_2 on the rGO sheets. Biological assays demonstrated significant antimicrobial activity against both Gram-positive and Gram-negative bacterial strains, as well as selected fungal species. Notably, enhanced inhibition was observed against Gram-positive bacteria, which may be due to the synergistic interaction between the components of the nanocomposite. Overall, the study highlights the potential of rGO/Fe_3O_4/SnO_2 nanocomposites as promising candidates for sustainable and effective water purification systems, targeting microbial contamination.

1 INTRODUCTION

Nanocomposites of rGO, Fe_3O_4, and SnO_2, among many others have been prioritized. This is viewed as convincing evidence of their increasing place in modern nanotechnological applications regarding environmental remediation, especially around water treatment [1], [2]. Indeed, in microbial contamination, these materials hold much promise when considered for use in problems regarding public health [3]. The rGO/Fe_3O_4/SnO_2 nanocomposite has a synergetic combination of properties enhancing its biological activity. SnO2 offers a source of enhanced antimicrobial activity because it can efficiently produce reactive oxygen species (ROS) [4]. These ROS can effectively damage the microorganism's cell wall and cellular-internal components upon irradiation with light. Meanwhile, rGO provides a higher surface area and ease of adsorption of microbial contamination [5], [6]. Fe_3O_4 is responsible for its magnetic property, which can make recovery easy from an aqueous system. SnO_2 is also well-known to be highly antimicrobial because it can effectively cause the generation of reactive oxygen species (ROS) [7]. The biological activity of the rGO/Fe_3O_4/SnO_2 nanocomposite sets it apart in wide applicability against different microorganisms like bacteria and fungi responsible for contamination; hence, it provides lower risks of waterborne infections through the control of bacterial and fungal contamination [8], [9]. This study reports the synthesis characterizations of rGO/Fe_3O_4/SnO_2 nanocomposite and their evaluation of biological activity applicable to water treatment [10]. The work will be carried out in pursuit of addressing microbial contamination which is still one of the major challenges toward ensuring accessibility to clean drinking water [11].

2 EXPERIMENTAL PART

The $rGO/Fe_3O_4/SnO_2$ nanocomposite was synthesized using Hummer's method, the nanocomposite was synthesized using the co-precipitation method [12].

3 RESULTS AND DISCUSSION

3.1 Characterization of $rGO/Fe_3O_4/SnO_2$

The FT-IR, XRD, FESEM, and EDX were used for the characterization of the synthesized samples. FT-IR spectra have confirmed the formation of nanoparticles of material composites. Surface morphology and nanoparticle size were determined by FESEM. The characteristics of the $rGO/Fe_3O_4/SnO_2$ nanocomposite powder used in this work were studied by XRD, and qualitative analysis was done by EDX to establish the elemental composition of the samples.

3.2 FT-IR Spectrum of $rGO/Fe_3O_4/SnO_2$

The IR spectrum of the $rGO/Fe_3O_4/SnO_2$ composite presents some most salient peaks which can be used to affirm the successful synthesis and incorporation of rGO, Fe_3O_4, and SnO_2. The broad peak centered at 3424 cm^{-1} is associated with O-H stretching vibrations, pointing towards adsorbed water molecules or hydroxyl groups on the substance surface. A peak located at 1610 cm^{-1} gives the stretching vibrations for C=C, thus conformity to the presence of sp^2-hybridized carbon domains in rGO. Peaks near 1444 cm^{-1} may relate to bending vibrations of functional groups on the composite surface. The peak at 1151 cm^{-1} is associated with C-O stretching, indicating residual oxygen-containing groups on the rGO surface. The vibrational bands in the range of 800–400 cm^{-1} confirm the existence of Sn-O and Fe-O bonds. Notably, the band around 606 cm^{-1} can be attributed to Fe-O vibrations within the Fe_3O_4 lattice, while the peak at 412 cm^{-1} is characteristic of Sn-O stretching vibrations in SnO_2 as shown in Figure 1.

3.3 FESEM of $rGO/Fe_3O_4/SnO_2$

The FESEM micrograph shows the nanoscale morphology of an $rGO/Fe_3O_4/SnO_2$ composite material. The sheet-like structure of rGO is evident, serving as a conductive matrix, while Fe_3O_4 and SnO_2 nanoparticles are distributed on their surface. The marked measurement (43.46 nm) confirms the nanoscale features, essential for enhanced performance in applications such as energy storage or sensing. The smooth rGO sheets indicate an effective reduction, while irregularities suggest successful nanoparticle deposition. This composite demonstrates a well-engineered structure with potential for advanced technological applications as shown in Figure 2.

3.4 XRD Analysis of $rGO/Fe_3O_4/SnO_2$

The analysis of XRD data for the $rGO/Fe_3O_4/SnO_2$ composite confirms the presence of its key phases. The broad peak at 20.5251° indicates the amorphous nature of rGO due to structural defects. The peaks at 26.8778°, 34.2140°, and 52.1276° confirm the well-crystallized rutile tetragonal phase of SnO_2. Additionally, peaks at 31.2697° and 38.2429° validate the cubic spinel structure of Fe_3O_4. This combination of phases demonstrates the successful synthesis of the composite as shown in Figure 3.

3.5 EDX Analysis of $rGO/Fe_3O_4/SnO_2$

The EDX data confirms the composition of the $rGO/Fe_3O_4/SnO_2$ composite, showing contributions from carbon (C) primarily from rGO, oxygen (O) from Fe_3O_4 and SnO_2, iron (Fe) from Fe_3O_4, and tin (Sn) from SnO_2. The weight percentages sum to 100%, with carbon being the most abundant element by atomic percentage, indicating the prominence of rGO. The standards are used to ensure accurate calibration. The composition aligns with the expected properties of the composite, where rGO improves conductivity, Fe_3O_4 adds magnetic properties, and SnO_2 contributes to catalytic or sensing functions as shown in Table 1 and Figure 4.

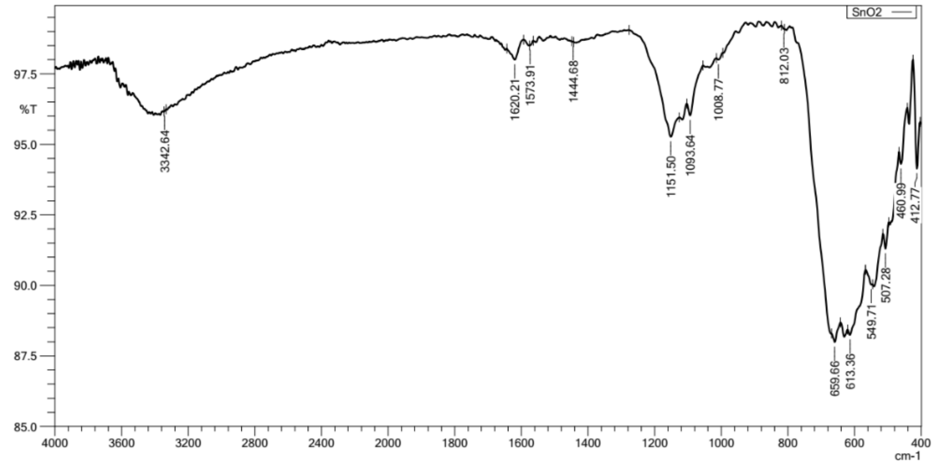

Figure 1: FTIR chart for rGO/Fe_3O_4/SnO_2.

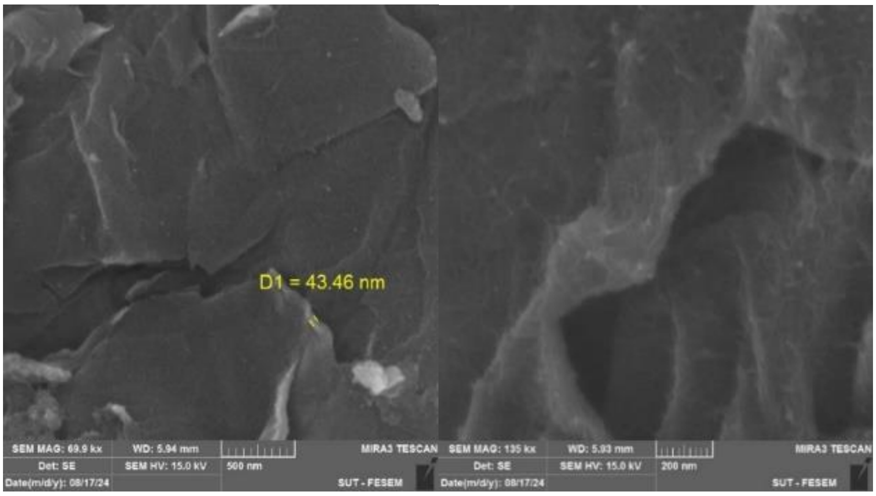

Figure 2: FESEM of rGO/Fe_3O_4/SnO_2.

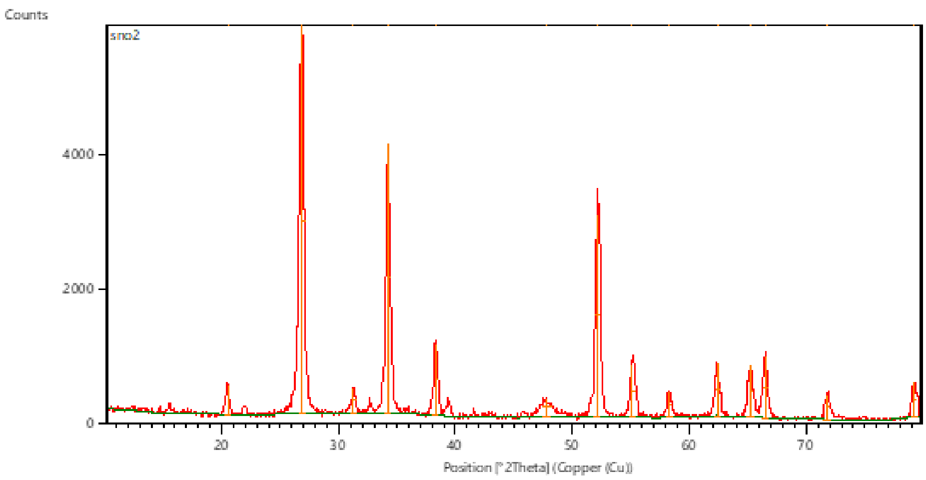

Figure 3. XRD analysis of rGO/Fe_3O_4/SnO_2.

Table 1: EDX analysis of rGO/Fe_3O_4/SnO_2.

Element	Line Type	Apparent Concentration	k Ratio	Wt%	Wt% Sigma	Atomic %
C	K series	1.38	0.0138	29.06	0.30	56.68
O	K series	1.70	0.0057	19.29	0.26	28.25
Fe	K series	2.60	0.026	21.96	0.28	9.21
Sn	L series	3.05	0.031	29.69	0.28	5.86
Total:				100.00		100.00

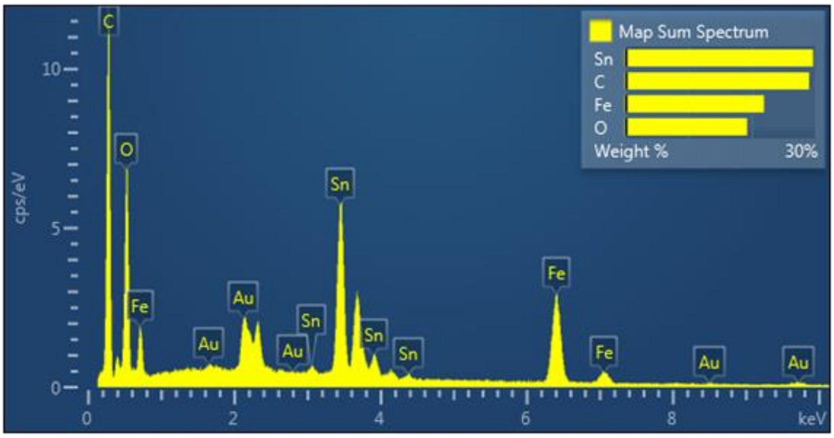

Figure 4: EDX analysis of rGO/Fe_3O_4/SnO_2.

4 BIOLOGICAL ACTIVITY

4.1 Identified Pathogens in Tannery Wastewater

Tannery wastewater is a major public health concern. To control contamination risks, it is necessary that appropriate treatment and monitoring conditions are maintained [13]. For isolation of Aspergillus spp., the principle includes the plating of the samples on PDA, a medium rich in nutrients and supportive to the growth of fungi. After incubation at 25°C for 7 days, the colonies of the fungi are assessed based on their microscopic appearances of colors, smooth or rough textures, and patterns of sporulation. The identity of the species is confirmed based on molecular and microscopic techniques, and thus more accuracy is ensured. Agar well diffusion sensitivity testing of bacteria are used to assess the efficacy of the extract. Bacteria of the order of magnitude of 1.0 x 10^8 cells per milliliter are spread onto Mueller Hinton Agar, and the wells are filled with concentrations of the extract and positive control. The plates are then incubated at 37 degrees Celsius for a period of 18-24 hours, after which time the zones of inhibition are measured so that the antimicrobial activity can be determined. Bacillus spp. from tannery effluents becomes a major health hazard with bacterial counts ranging from 10^6 to 10^9 CFU/mL. Toxins produced by pathogenic strain B. cereus cause gut-related infections, skin infections, and in rare cases, septicemia. There is a need for proper monitoring and treatment of waste to mitigate this potential risk.

Pseudomonas aeruginosa is isolated on Pseudomonas agar, which is a selective medium for adjustment to pH 7.0 ± 0.2. After 24-48 hours of incubation at 35-37°C, the bacteria metabolize and raise the pH, turning the color of agar to purple. This is only a preliminary indicator for P. aeruginosa. But, much more important is that some biochemical testing needs to be done for further confirmation. Biofilm formation by this pathogen proves to be rampant in the resistance of treatment, an aspect that calls for a very healthy monitoring system as well as wastewater management. Health problems associated with bacterial contamination of tannery wastewater are dire at bacterial concentrations within the range of 10^6 and 10^9 CFU/mL. Streptococcus pyogenes is quite dangerous; it attacks the skin and respiratory system leading to necrotizing fasciitis plus Streptococcal Toxic Shock Syndrome (STSS). This risk must be minimized via proper practices in wastewater treatment procedures.

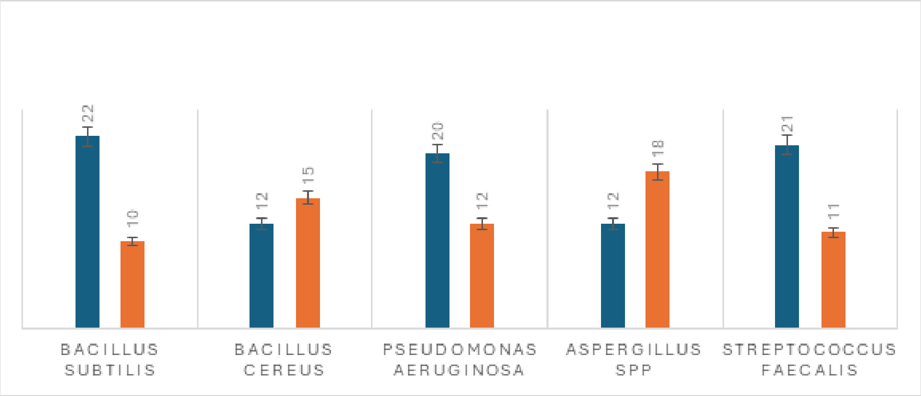

Figure 5: Antimicrobial activity of $rGO/Fe_3O_4/SnO_2$ nanocomposite against selected microorganisms.

Pseudomonas aeruginosa has an immense effect on the effluents from tanneries at concentrations of 500 CFU/mL. These concentrations are relatively high and permit it to cause skin infection, respiratory condition, systemic infection, especially in immunocompromised people. Biofilm makes it hard to treat; hence, this gives a quick call for good waste control. Aspergillus spp. has a serious pathogenic health effect in tannery wastewater, considered as a potent mycotoxin producer of aflatoxin B1. High concentrations of fungi in contaminated water pose an increased risk of respiratory reaction, asthma, allergy, and aspergillosis to humans; skin disease and systemic toxicity can also result from exposure. Effective monitoring of the fungi and strong waste treatment are found to be very important to keep contamination diseases away. Stronger waste management is very important to reduce contamination risks, better public health, and brown environmental conditions [14].

4.2 Effect of $rGO/Fe_3O_4/SnO_2$ Nanocomposite on Various Microorganisms

The activity of $rGO/Fe_3O_4/SnO_2$ nanocomposite against antimicrobial proves that the nanocomposite caused differential growth of microorganisms. A minimum inhibitory concentration (MIC) of 10 mg/mL and an inhibition zone of 22 mm indicate that SnO_2 has moderate susceptibility towards a Gram-positive bacterium, Bacillus subtilis. SnO2 nanoparticles have low MIC at 11 mg/mL and moderate susceptibility (with an inhibition zone of 21 mm) to Streptococcus faecalis. The difference in their sensitivity is also manifested by Bacillus cereus fringe inhibition values of 12 mm and the highest MIC of 15 mg/mL, respectively, thereby indicating much higher resistance compared to B. subtilis and S. faecalis. P. aeruginosa, being a Gram-negative bacterium, has slightly less sensitivity and an MIC of 12 mg/mL with a 20-mm inhibition zone probably as a response to the difficulty in the passage of nanoparticles to the other side, which is regulated by the existence of an outer membrane. Typical of Aspergillus spp. It had no sensitivity, only an inhibition zone of 12 mm and a high MIC at 18 mg/mL. This indicates the complex composition of the fungal cell wall, which does not allow nanoparticles to be effective. Overall, $rGO/Fe_3O_4/SnO_2$ nanocomposite appears more active, primarily against Gram-positive bacteria, such as Bacillus subtilis and Streptococcus faecalis, but much less active against Gram-negative bacteria and fungi. Such results indicate that SnO_2 nanoparticles hold promise for infections with Gram-positive bacteria and require in-depth further optimization for effective applications against other microbes [10] as shown in Figure 5.

5 CONCLUSIONS

The synthesis and characterization of rGO/Fe3O4/SnO2 nanocomposites were conducted successfully; hence, they show exciting potential for biological applications in water treatment. These composites provide a unique combination of the properties of reduced graphene oxide, magnetic iron oxide, and tin dioxide to ensure that microbial contamination, especially Gram-positive bacteria, is successfully dealt with. Results of this study confirmed the strong antimicrobial activity of the composite, characterized by clear inhibition zones and low MIC values in the challenge pathogens therefore qualifies it for use in reducing health risks associated with contaminated water. Though showing good antimicrobial behavior against bacteria, the low activity observed against fungi and Gram-negative bacteria opens more avenues for optimization in the future. In sum, this work highlights the sustainability and dependability of $rGO/Fe_3O_4/SnO_2$ nanocomposites as a multifunctional implement for environmental remediation on the part of the broader imperative of access to clean and safe water.

ACKNOWLEDGMENTS

The authors thank the Department of Chemistry, College of Education for Pure Sciences/Ibn Al-Haitham, University of Baghdad, for providing chemicals and support.

REFERENCES

[1] M. A. Ahmed, M. A. Ahmed, and A. A. Mohamed, “Facile adsorptive removal of dyes and heavy metals from wastewaters using magnetic nanocomposite of zinc ferrite@reduced graphene oxide,” Inorg Chem Commun, vol. 144, 2022, doi: 10.1016/j.inoche.2022.109912.

[2] A. Abdul, R. Nemea, and B. I. Al-Abdaly, “Synthesis and Characterization Two Nanocomposites of Fe3O4 Nanoparticles and Using Them as a Chemical Sensors,” Ibn Al-Haitham Journal for Pure and Applied Sciences, no. 37(3), 2024, doi: 10.30526/37.3.3293.

[3] K. T. Lafta and T. A. Salman, “Green Synthesis, Characterization of Copper Sulfide Nanoparticles and Antibacterial Activity Evaluation,” Iraqi Journal of Science, vol. 65, no. 11, pp. 6277–6287, 2024, doi: 10.24996/ijs.2024.65.11.7.

[4] T. A. Naif and B. J. Ahmed, “Ibn Al-Haitham Journal for Pure and Applied Sciences Synthesis, Characterization and Study of the Effect of Nanoparticles on the Biological Activity of New Silicon Polymers and Their Nanocomposites,” 2024, doi: 10.30526/37.4.3391.

[5] M. Abdulsatar Abduljabar and S. H. Merza, “Synthesis, Characterization of Nickel Cobaltite Nanoparticles and Its Use in Removal Methyl Green Dye from Aqueous Solution,” 2024, doi: 10.30526/37.3.3398.

[6] Y. M. Sadiq and E. E. Al-Abodi, “Preparation and characterization of a new nano mixture, and its application as photocatalysis in self-assembly method for water treatment,” in AIP Conference Proceedings, 2019. doi: 10.1063/1.5138528.

[7] L. Musab and E. E. Al-Abodi, “Preparation and characterization composites contain of magnetic iron oxide nanoparticles with different weight ratios of dextrin and using it to removal of heavy metals from aqueous solutions,” in Energy Procedia, 2019. doi: 10.1016/j.egypro.2018.11.241.

[8] D. J. Hadi and M. A. Younus, “Bio Synthesis, Characterization, and Evaluation of the Anticancer Activity of Gold and Silver Nanoparticles and Their Polyacetal Nanocomposite,” Iraqi Journal of Science, vol. 65, no. 12, pp. 6824–6841, 2024, doi: 10.24996/ijs.2024.65.12.4.

[9] A. A. Shareef, Z. A. Hassan, M. A. Kadhim, and A. A. Al-Mussawi, “Antibacterial activity of silver nanoparticles synthesized by aqueous extract of Carthamus oxycantha M.Bieb. Against antibiotics resistant bacteria,” Baghdad Science Journal, vol. 19, no. 3, pp. 460–468, 2022, doi: 10.21123/BSJ.2022.19.3.0460.

[10] K. Hadi and T. M. Al- Saadi, “Investigating the Structural and Magnetic Properties of Nickel Oxide Nanoparticles Prepared by Precipitation Method,” Ibn AL-Haitham Journal for Pure and Applied Sciences, vol. 35, no. 4, 2022, doi: 10.30526/35.4.2872.

[11] D. John, J. Jose, S. G. Bhat, and V. S. Achari, “Integration of heterogeneous photocatalysis and persulfate based oxidation using TiO2-reduced graphene oxide for water decontamination and disinfection,” Heliyon, vol. 7, no. 7, 2021, doi: 10.1016/j.heliyon.2021.e07451.

[12] A. F. Ismail and E. E. Al-Abodi, “Synthesis and Characterization of rGO/Fe3O4/SnO2 Nanocomposite to Remove Terasil Black Dye from Aqueous Solutions,” Advanced Journal of Chemistry, Section A, vol. 8, no. 4, pp. 687–699, Apr. 2025, doi: 10.48309/ajca.2025.476649.1669.

[13] M. Rezayat, M. Karami Moghadam, M. S. Yazdi, M. Moradi, and M. Bodaghi, “Statistical analysis of experimental factors for synthesis of copper oxide and tin oxide for antibacterial applications,” International Journal of Advanced Manufacturing Technology, vol. 127, no. 5–6, 2023, doi: 10.1007/s00170-023-11728-z.

[14] S. Rehman et al., “Biocompatible Tin Oxide Nanoparticles: Synthesis, Antibacterial, Anticandidal and Cytotoxic Activities,” ChemistrySelect, vol. 4, no. 14, 2019, doi: 10.1002/slct.201803550.